Study on Aging and Recover of Poly (Lactic) Acid Composite Films with Graphene and Carbon Nanotubes Produced by Solution Blending and Extrusion

Rumiana Kotsilkova [1],*, Polya Angelova [1], Todor Batakliev [1], Verislav Angelov [1], Rosa Di Maio [2] and Clara Silvestre [2],*

[1] Institute of Mechanics, Bulgarian Academy of Sciences, 1113 Sofia, Bulgaria; polq_s_angelova90@abv.bg (P.A.); todorbat@gmail.com (T.B.); verislav@abv.bg (V.A.)
[2] Institute of Polymers, Composites and Biopolymers, CNR, Via Campi Flegrei, 34, 80078 Pozzuoli (NA), Italy; rosadimaio1988@libero.it
* Correspondence: kotsilkova@yahoo.com (R.K.); clara.silvestre@ipcb.cnr.it (C.S.)

Abstract: The aging, annealing, and reprocessing of the biodegradable poly (lactic) acid (PLA) based composite films incorporating graphene and carbon nanotubes were investigated in this work. Various monofiller and bifiller nanocomposite films with 6 wt.% filler content were produced by a solution-phase technique followed by extrusion. The freshly produced films were compared with the aged films after 18 months of shelf life in a room environment. The effects of aging, annealing, and melt reprocessing on the crystalline structure, the thermal stability, the hardness, and Young's modulus were analyzed by differential scanning calorimetry (DSC), TGA, and nanoindentation methods. The fresh and the aged samples were found to have semi-crystalline materials with 3%–7% crystallinity, while the crystallinity was significantly enhanced to 34%–38% by annealing at 80 °C and subsequent slow cooling. A good dispersion was observed in the bifiller films with filler ratios of 4.5:1.5 and 1.5:4.5 [graphene nanoplatelets (GNP) to carbon nanotubes (CNT)], which affected the crystallization processes. The reprocessing at 200 °C followed by fast cooling resulted in amorphous films, which significantly reduced the hardness and Young's modulus. The nanoindentation properties were dependent on the dispersion of nanofillers at the surfaces. The efficiency of annealing and reprocessing for the recovery and the reuse of aged nanocomposite films is discussed herein. The paper underlines that properties of the nanocomposites under investigation were influenced not only by the composition, the chemical nature of the added filler, and the processing condition, but also by the aging processes, which in turn depended on the type of nanopartcles added to PLA and the compositions. The paper provides valuable information for selection of material and processing conditions.

Keywords: PLA; graphene; carbon nanotubes; aging; reprocessing; crystallinity; thermal properties; nanoindentation

1. Introduction

For the proper use of biodegradable poly (lactic) acid (PLA) based films, it is important to determine the changes of structure, morphology, and properties during storage and reprocessing. It is well known that PLA with different degrees of crystallinity can be obtained by varying processing and crystallization conditions. Totally amorphous PLA products were reported [1–4] if produced by injection molding due to the high cooling rates compared to the low PLA crystallization rate.

PLA is characterized by a polymorph structure. During annealing at temperatures of 130–140 °C in PLA-based polymers, the disordered α crystalline form, which can be produced by annealing at lower temperatures, transforms into the ordered α' form [4]. The two processes—the melting of the α' form and the recrystallization into the α form—are considered as the α'-α phase transition [5,6]. Crystallinity has been found to influence the dynamic mechanical properties. Thus, if the recrystallization occurs above the glass transition, this could increase the storage modulus [7]. Recrystallized PLA products demonstrate much higher heat deflection temperatures for the semi-crystalline PLA products compared to the amorphous PLA products [8]. Toughness improvement of PLA by control of crystallinity is of crucial importance, as PLA is a very brittle material with less than 10% elongation at break [9,10]. Researchers found that thermo-mechanical processing as injection molding and extrusion led to the quasi-disappearance of the crystal structure, whereas it was recovered after annealing [11]. Extruded materials showed a significant increase in elongation at break (32%–35%) compared to injected materials, and it was attributed to a higher number of chains due to chain scissions in reprocessed materials. After annealing, samples showed increased Young's modulus and yield strength and reduced gas permeability due to the increased crystallinity of annealed materials and the subsequent decrease in chain mobility. However, the products shrank and significant warpage occurred during recrystallization due to the increasing crystallinity [4]. Authors reported that distortion-free semi-crystallized PLA products could only be made during the process using nucleating agents [8,12].

The performance of the biodegradable PLA polymer in terms of durability is limited by complex aging mechanisms, including thermal decomposition, hydrolysis, oxidation, and natural weathering [9–11,13,14]. The degradation rates have been found to depend on PLA crystallinity, molecular weight distribution, morphology, and water diffusion rates into the polymer [9]. At atmospheric conditions, authors found that the degradation rate of PLA was slow, and this led to a long lifetime, which could have been up to 3–5 years. Therefore, the PLA composite materials and the products that are intended for long-term use should be tested in real time and with realistic in-service environments [14]. However, such studies are rarely reported because the time involved would significantly delay product development. No studies are reported on aging during storage in room conditions, which is of big importance for the shelf life of the PLA-based composite films and products.

Nanosize additives in PLA polymers were recently used to achieve specific properties by providing nucleation agents to initiate crystallization [15–17]. Authors reported that carbon nanotubes (CNTs) and graphene nanoplatelets (GNPs) may have enhanced the nucleation rate of polylactide [18–22]. It was observed that the melt crystallization behavior of PLA depended strongly on the presence of GNPs, which dominantly acted as heterogeneous nucleating agents and increased the crystallization rate compared to the neat PLA [20]. However, the crystallinity began to decrease at higher cooling rates and higher GNP content due to the slowly crystallizing PLA polymer and the GNPs aggregation effect [21]. A comparative crystallization study on PLA composites filled with CNTs and GNPs found that both nanofillers acted as heterogeneous nucleation agents; however, the induction ability of CNTs was stronger than that of GNPs [22]. The filer loading in conjunction with annealing may have significantly affected melting behavior, glass transition temperature, and properties of PLA, producing higher crystallinity and enhanced Young modulus, impact strength, flexural modulus, and stiffness [23–28].

There is a need for further research in this area, including the effect of aging and the recovery of aged nanocomposite films with selected properties. It is well known that the selection of polymers for use as specific materials requires the consideration of how these will withstand the environmental conditions to which they will be subjected. This is particularly true for PLA-based materials, as this polymer, if cooled during the processing to below its glass transition, presents a high amount of amorphous material that can undergo small-scale relaxation processes, causing a significant change in macroscopic properties at room temperature. A wide range of materials is affected by this aging at room temperature, and extensive studies have been carried out on homopolymers and copolymers.

Contrary to this, less attention has been devoted to the change in properties of polymer nanocomposites due to the aging process.

This paper is devoted to filling this gap by investigating the fresh and the aged PLA composite films filled with 6 wt.% graphene, CNTs, and their combinations. The PLA-based films were aged by 18 months of storage in a room environment. Structural changes and thermal and surface mechanical properties of the nanocomposite films were investigated by performing TEM, differential scanning calorimetry (DSC), TGA, and nanoindentation tests. The effects of annealing and melt reprocessing on the crystal structure and the thermal and nanomechanical properties of the aged nanocomposite films were evaluated in order to propose a tool for the recovery and the reuse of aged film.

2. Materials and Methods

2.1. Materials

The PLA, Ingeo 700 1D from NatureWorks, Blair, Nebraska, USA, was used as a matrix polymer. GNPs (with purity > 99.5 wt.%, thickness 4–20 nm, median size 5–7 µm) and multiwalled CNTs (purity > 95%, outer diameter > 50 nm, and length 1–5 µm) were supplied from Times Nano, Chengdu, China. The nanocomposite materials were fabricated by a solution blending processing technique, where the PLA was dissolved in chloroform in a ratio of 1:3, and suspensions of GNP and CNT in chloroform were prepared by ultrasonic mixing and were then added to the dissolved PLA. The mixtures were mechanically stirred for 60 min and dried in a vacuum oven for 24 h at 80 °C. Then, the dried nanocomposite material was extruded by a 10 mm twin screw extruder Microlab (Rondol, Nancy, France) at 10 rpm within temperatures of 150–160 °C to film sheets of thickness of 0.1 mm. Monofiller and bifiller composite films containing 6 wt.% filler content of GNP, CNTs, and mixed fillers were produced. The following samples were prepared for further study: neat PLA and PLA with 6 wt.% filler content of GNP, CNT, and their mixtures of ratios: 6:0, 4.5:1.5, 3:3, 1.5:4.5, 0:6 GNP:CNT.

The nanocomposite films right after production were characterized as "fresh". Then, the films were "aged" for 18 months in storage in room conditions of an ambient temperature of 25 °C and a relative humidity of about 60%. The aged films were further processed by undergoing an annealing process by heating at 80 °C for 4 h and then slow cooling. These samples were labeled as "annealed". Additionally, the aged films were heat treated to melt at 200 °C and fast cooled in order to simulate the reprocessing, such as hot pressing, or recycling. These samples were labeled as "reprocessed".

2.2. Experimental Methods

Morphological analysis of the film samples obtained by solution blending followed by extrusion were performed in order to state the degree of dispersion of the fillers in the PLA matrix in the starting materials as functions of filler types and compositions. Bright field TEM analysis was performed on a FEI TECNAI G12 Spirit-Twin (LaB6 source, Hillsboro, OR, USA) equipped with a FEI Eagle-4k CCD camera operating with an acceleration voltage of 120 kV. Before the analysis, sections of the samples were realized at room temperature on a Leica EM UC6/FC6 ultramicrotome (Wetzlar, Germany) and placed on 400 mesh copper grids.

Study on crystallization and thermal properties was carried out with a differential scanning calorimeter DSC-Q20 (TA Instruments, New Castle, DE, USA) that monitored heat effects associated with phase transitions of the polymer as a function of temperature. The test was performed in two heating runs, as 5–8 mg of the sample were encapsulated in alumina pans and heated from 30 to 200 °C (first run), then kept at this temperature for 3 min and cooled to 30 °C followed by the second heating run and subsequent cooling. Two regimes of heating and cooling were applied in order to study the crystallization processes in the PLA-based composites: (i) heating at 20 °C/min with subsequent fast cooling at 20 °C/min, as well as (ii) heating at 10 °C/min and slow cooling at 1 °C/min for the "annealed" samples (performed by a controlled vacuum oven). From the DSC thermograms, the glass transition temperature (T_g), the cold crystallization temperature (T_{cc}), the melting temperature (T_m),

and their enthalpies, (ΔH_{cc}) and (ΔH_m), were determined, while the crystallization temperature (T_c) was determined from cooling of the melt. Taking into account that the PLA underwent cold crystallization during the DSC scan, the degree of crystallinity (χ_c) of the solution blended PLA-composite films was calculated based on the enthalpy value of a 100% crystalline PLA [3,12] from the following equation:

$$\% \text{ crystallinity } (\chi_c) = \left(\frac{\Delta H_m - \Delta H_{cc}}{w \Delta H_m^0} \right) * 100 \ (\%) \tag{1}$$

where ΔH_m is fusion/melting enthalpy (J/g), ΔH_{cc} is the cold crystallization enthalpy (J/g), w is the portion of the polymer in the composite, and ΔH_m^0 (93 J/g) is the melting enthalpy when the crystallinity of PLA is 100%. This approximate equation can provide information on the crystallinity of the sample removing the effects due to cold crystallization during the DSC scan.

Thermogravimetric analysis was performed by TGA-Q50 (TA Instruments) by heating from 30 to 500 °C with a ramp for 10 °C/min, under nitrogen flow. Characteristic temperatures such as the initial decomposition temperature (T_{onset}) and the decomposition peak temperature (T_p) as well as the residue ash at the end of heating (490 °C) were determined. The weight loss at 105 °C was evaluated in order to determine the amount of absorbed humidity in the film material.

Nanoindentation measurements were made using an indenter type Berkovich Diamond with a tip radius of 70 nm in the force control mode of 100 mN. Load was measured as a function of penetration depth. Each test was repeated 48 times (4 × 12; spacing between indents 80 μm) to have statistical data. Test samples were prepared by diamond knife cuts of 0.1 μm thick sheets. A typical indentation experiment consists of the following steps: (i) approaching the surface, (ii) loading to the peak load of 100 mN for 15 s, (iii) holding the indenter at peak load for 10 s, (iv) unloading from maximum force of 100 mN to 10% for 15 s, (v) holding at 10% of max force for 15 s, and (vi) final complete unloading for 1 s (load function 15 s–10 s–15 s trapezoid). The hold step was included to avoid the influence of the creep on the unloading characteristics, since the unloading curve was used to obtain the elastic modulus of the material. The Oliver-Pharr method [29] was used for calculation of the nanoindentation hardness and Young's modulus.

3. Results

3.1. Morphology

Figure 1a–f displays TEM micrographs for the neat PLA and the composite films with 6 wt.% filler content of GNP, CNT, and their combinations in different ratios of: 6:0, 0:6, 1.5:4.5, 4.5:1.5, and 3:3, GNP:CNT, respectively. The neat PLA film in Figure 1a is transparent with absence of any ingredients. Totally different filler dispersity and structure was obtained depending on the composition. The monofiller films, 6GNP/PLA and 6CNT/PLA, in Figure 1b,c shows poorly dispersed nanofillers with large aggregates of sizes from 100 nm to 1 μm and above, which had anysotropic shapes in the case of graphene. By adding CNTs as a second filler, the dispersion of both fillers was strongly improved, particularly for the ratios 4.5GNP/1.5CNT (Figure 1d) and 1.5GNP/4.5CNT (Figure 1e), where the GNPs were dispersed to a few layers of nanoplatelets with median size of few μm, and the CNTs were seen as single nanotubes or fine agglomerates. However, at an equal ratio for both fillers in the bifiller composite, 3GNP/3CNT (Figure 1f), the GNPs and the CNTs showed a tendency to form small agglomerates in the PLA matrix.

In order to visualize the degree of dispersion of the combined fillers (GNP and CNT in the PLA matrix at nanoscale), Figure 2a–c presents the TEM micrographs of the bifiller composite films at higher magnification. Thus, in Figure 2a,b, the bifiller composites, 4.5GNP/1.5CNT and 1.5GNP/4.5CNT, demonstrated very good exfoliation of graphene to few layers, while the CNTs were dispersed mostly to single nanotubes in the volume by the filler ratios of 4.5:1.5 and 1.5:4.5 (GNP:CNT). However, at the bifiller composite, 3GNP/3CNT (shown in Figure 2c), the CNTs were seen to be attracted on the surfaces

of the GNPs and had formed joint agglomerates of 50–500 nm in size. Thus, the dispersion of both fillers in PLA was worsened by the equal filler ratio of 3:3 (GNP:CNT).
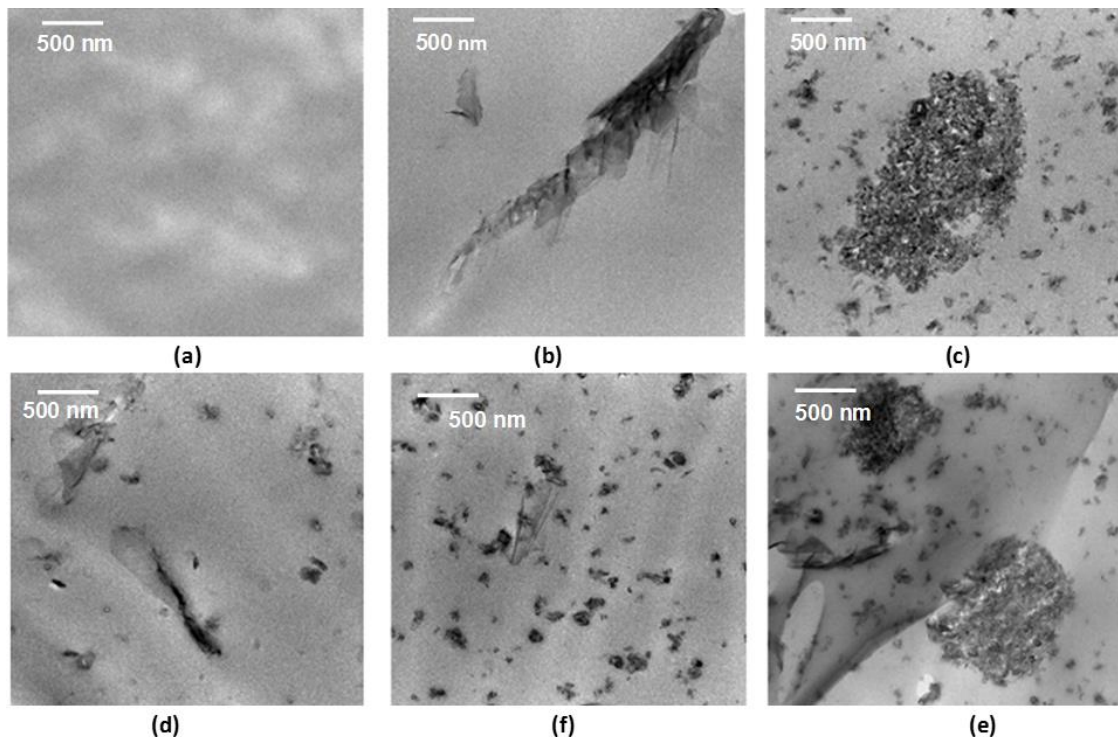

Figure 1. TEM micrographs of 6 wt.% monofiller and bifiller composite films, varying the types and the combinations of carbon fillers: (**a**) neat poly (lactic) acid (PLA); (**b**) 6 graphene nanoplatelets (GNP)/PLA; (**c**) 6 carbon nanotubes (CNT)/PLA; (**d**) 4.5GNP/1.5CNT/PLA; (**e**) 1.5GNP/4.5CNT/PLA; and (**f**) 3GNP/3CNT/PLA.
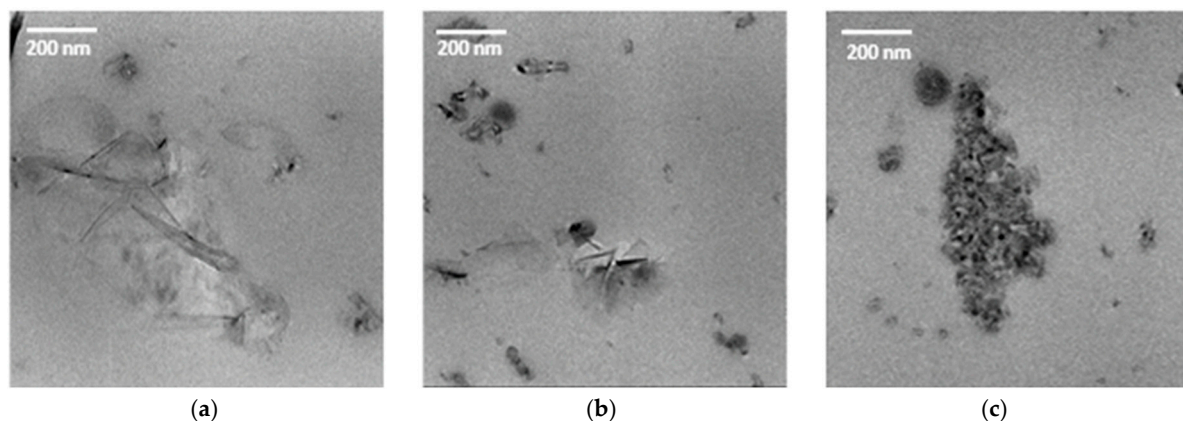

Figure 2. TEM micrographs of the bifiller composite films at high magnification, as indicated by the bar: (**a**) 4.5GNP/1.5CNT/PLA; (**b**) 1.5GNP/4.5CNT/PLA; and (**c**) 3GNP/3CNT/PLA.

It is not easy to explain the improvement of the dispersion of both fillers by introducing the second filler. In order to make a hypothesis, the improvement could have been related to a repulsive effect between the two fillers that tended to distribute themselves as far as possible from each other, analogous to what was reported for some blends containing a copolymer, which were found miscible without any specific interaction because of the repulsion between the two different monomers constituting the copolymer [30].

3.2. Thermal Properties and Crystallinity of Fresh and Aged Composite Films

The effect of 6 wt.% nanofillers (GNP, CNT, and their mixtures) on the PLA thermal properties was investigated for the "fresh" prepared films and the "aged" films after 18 months of storage in room conditions. The "as received" nanocomposite films were studied by analyzing the DSC thermograms from the first heating run carried out at a heating rate of 20 °C/min. We analyzed the DSC first heating run in order to obtain information about the effects of thermal history for the fresh films related to processing and cooling, as well as the effect of aging related to absorption of humidity and partial degradation of the PLA. In Figure 3a,b, the DSC curves of heat flow versus temperature are presented, where the freshly prepared films (in Figure 3a) are compared with the aged films (in Figure 3b). The thermal and the crystallization characteristics are summarized in Table 1.
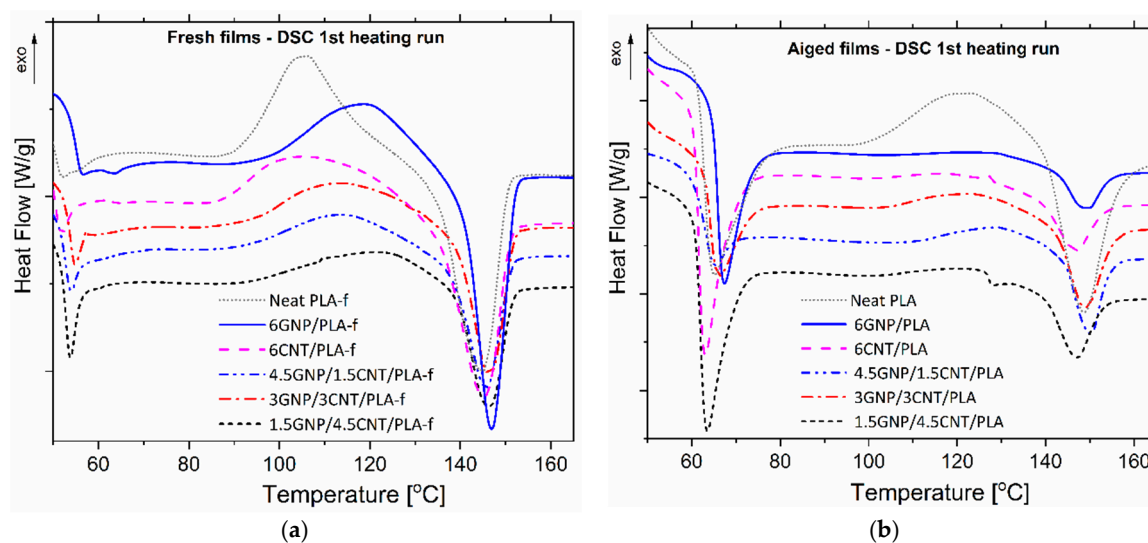

Figure 3. Differential scanning calorimetry (DSC) thermograms in the first run at a heating rate of 20 °C/min for the PLA and 6 wt.% composite films, varying the filler combinations. Comparison between: (**a**) freshly prepared films, and (**b**) aged films after 18 months of storage.

Typically, the DSC curves for the neat PLA and the nanocomposites showed glass transition (T_g) followed by an exothermal peak of the cold crystallization (T_{cc}) and finally an endotherm peak (T_m) related to the melting of the crystals.

For the "fresh" films in Figure 3a, the effect of GNPs on the upper three characteristic temperatures was stronger than that of CNTs. A slight difference was observed in the value of the T_g for all samples. It could be noted that the presence of GNP in both binary and ternary mixtures always produced an increase in the T_g, indicating that the presence of the GNP platelet negatively influenced the mobility of the PLA chain. This hypothesis was confirmed by the higher T_{cc} of the films containing GNPs, e.g., the 6GNP/PLA-f sample presenting a T_{cc} of 15 °C higher than that of the 6CNT/PLA-f and the neat PLA (Table 1). A similar effect was observed in the bifiller composites with GNP and CNT, where the T_{cc} was shifted to higher temperatures by 6–13 °C compared to the neat PLA.

In contrast, different thermal behavior was observed for the "aged" nanocomposite films after storage for 18 months in room conditions, as shown in Figure 3b. The T_g of the aged films was 62–64 °C, which was a shift up of about 10 °C compared to that of the fresh films (50–54 °C). This increase could have been associated with the changes of conformation of macromolecules through spontaneous relaxation during the aging to reach the equilibrium state, which brought shrinkage of a specific volume, decreases in specific enthalpy and entropy, decreases in molecular mobility and free volume, and were reflected in the increase in T_g [31].

Table 1. DSC characteristic temperatures and crystallinity of fresh and aged composite films. Effects of solid annealing and melt reprocessing on thermal characteristics of aged films.

"Fresh" Films	DSC Results from First Heating Run at 20 °C/min					
	T_g, °C	T_{cc}, °C	T_m, °C	ΔH_{cc}, J/g	ΔH_m, J/g	χ_c, %
neat PLA-f	50.0	104.3	144.4	18.0	19.5	1.7
6GNP/PLA-f	54.1	119.3	147.0	11.7	14.4	3.0
6CNT/PLA-f	49.8	105.3	144.8	10.2	15.3	5.8
3GNP/3CNT/PLA-f	52.4	117.3	145.8	6.2	12.1	6.7
1.5GNP/4.5CNT/PLA-f	53.1	110.2	146.2	7.6	14.0	7.3
4.5GNP/1.5CNT/PLA-f	52.0	113.2	145.7	8.6	13.5	5.6

"Aged" Films for 18 Months Shelf Life at 25 °C	DSC Results from First Heating Run at 20 °C/min					
	T_g, °C	T_{cc}, °C	T_m, °C	ΔH_{cc}, J/g	ΔH_m, J/g	χ_c, %
neat PLA	62.6	119.4	148.5	7.7	7.9	0.2
6GNP/PLA	62.3	–	148.1	–	2.8	3.3
6CNT/PLA	61.3	127.3	146.5	–	3.6	4.1
3GNP/3CNT/PLA	63.7	123.5	148.7	1.8	5.0	5.7
1.5GNP/4.5CNT/PLA	61.7	125.3	146.8	–	4.9	5.6
4.5GNP/1.5CNT/PLA	63.9	120.8	150.2	5.4	10.4	5.7

"Annealed" Aged Films at 80 °C for 4 h	DSC Results from First Heating Run at 10 °C/min and Cooling at 1 °C/min						
	T_g, °C	T_{cc}, °C	T_m, °C	ΔH_{cc}, J/g	ΔH_m, J/g	χ_c, %	T_c, °C
neat PLA-ann	58	–	145.5	–	30.4	34.8	96.4
6GNP/PLA-ann	60	–	146.3	–	31.5	36.0	104.2
6CNT/PLA-ann	61	–	146.8	–	29.6	33.9	105.2
3GNP/3CNT/PLA-ann	61	–	146.9	–	30.4	34.8	105.6
1.5GNP/4.5CNT/PLA-ann	59	–	148.3	–	32.9	37.6	111.6
4.5GNP/1.5CNT/PLA-ann	60	–	147.2	–	29.6	33.9	116.9

"Melt reprocessed" Aged Films at 200 °C	DSC Results from Second Heating Run at 20 °C/min and Cooling at 20 °C/min						
	T_g, °C	T_{cc}, °C	T_m, °C	ΔH_{cc}, J/g	ΔH_m, J/g	χ_c, %	T_c, °C
neat PLA-re	62.9	–	151.3	–	0.5	0.5	–
6GNP/PLA-re	63.0	–	-	–	–	–	–
6CNT/PLA-re	62.6	–	150.2	–	–	-	–
3GNP/3CNT/PLA-re	63.9	–	150.9	–	0.6	0.7	–
1.5GNP/4.5CNT/PLA-re	62.0	129.0	150.1	1.6	3.5	2.2	–
4.5GNP/1.5CNT/PLA-re	63.3	128.2	150.1	11.0	14.7	3.4	–

A cold crystallization peak and exothermal (ΔH_{cc}) were visible only for the neat PLA. For other systems, there was a weak cold crystallization process, probably due to the simultaneous increase of T_g that decreased the window of the cold crystallization (T_{cc}-T_g) process and the presence of the nanoparticles that hindered the movements of the chains toward the growing nuclei.

Small differences in the degree of crystallinity were observed for the "fresh" and the "aged" films depending on composition, as seen in Table 1. For the "fresh" films, the % crystallinity (χ_c) of the neat PLA was calculated to be 1.7%, while it slightly increased to 3%–7% for the composite films containing GNPs and CNTs. This was probably due to a nucleating effect on PLA crystals of the GNP and the CNT fillers that promoted the PLA crystallization process. A decrease in crystallinity was observed for the "aged" neat PLA film to 0.2%, which was an indication for a partial PLA degradation due to the long-term exposure to ambient humidity, UV light, and room temperatures during the 18 month shelf life of the films. However, for the "aged" composite films, the percentage of crystallinity (χ_c, %) was insufficiently changed compared to the fresh films due to the presence of GNP and CNT fillers in the PLA matrix, which could obviously prevent the degradation process.

3.3. Annealing of Aged Nanocomposite Films

It is important to understand if annealing processes can influence the crystal structure of the "aged" PLA-based composite films in order to improve and recover their mechanical and thermal properties after long-term storage. Therefore, the "aged" composite films were "annealed" by heating at 80 °C for 4 h and then cooled slowly to room temperature in a vacuum oven. Figure 4 shows the DSC curves of the "annealed" aged films, thus the first heating run at a rate of 10 °C/min (Figure 4a), as well as the subsequent cooling of the melt at 1 °C/min after the first heating run (Figure 4b).
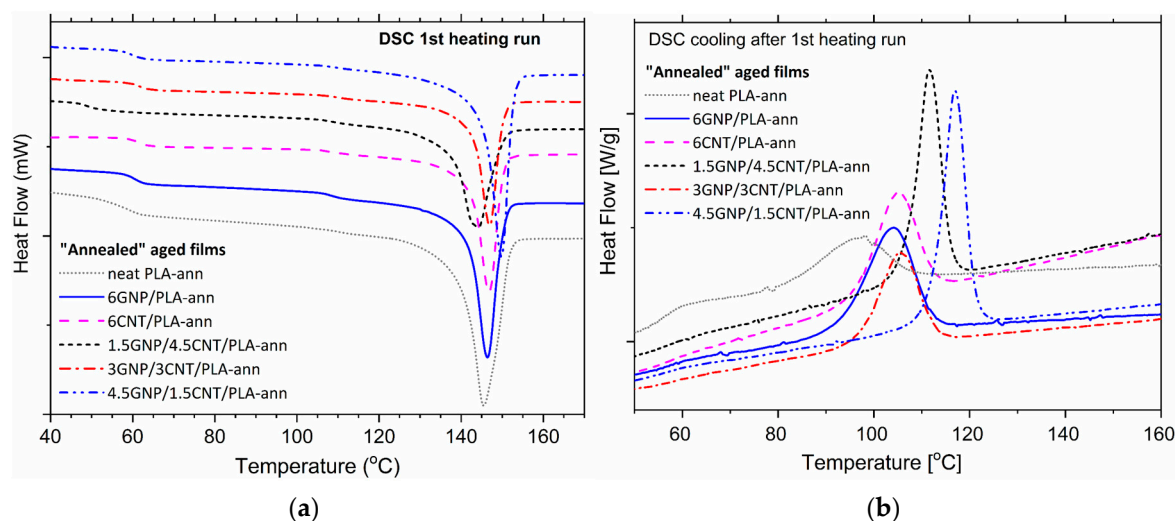

(**a**)　　　　　　　　　　　　　　　　　　　　　　　　(**b**)

Figure 4. DSC thermograms of the "annealed" aged films at 80 °C for 4 h: (**a**) first heating run at 10 °C/min, and (**b**) subsequent slow cooling of the melt at 1 °C/min after the first heating run.

From the obtained results in Table 1, it was possible to notice that the glass transition temperature (T_g) and the melting temperature (T_m) of the aged films were slightly reduced by 1–2 °C by annealing. The "annealed" aged samples in Figure 4a did not show cold crystallization, but an appreciable endothermic peak appeared during melting that was associated with the melting of more PLA crystals formed during annealing compared to that of the aged films before annealing (Figure 3b).

The slow cooling at 1 °C/min in Figure 4b confirmed the melt crystallization process of PLA at a slow rate, where the crystallization peak was shifted up with 8–9 °C for the monofiller composite films and for the bifiller films at a ratio of 3:3 compared to that of the neat PLA. This was indicative of the facilitated melt crystallization process by the presence of GNPs and CNTs due to the nucleation effect of the fillers. Importantly, the bifiller films of the filler ratio (4.5:1.5), particularly 4.5GNP/1.5CNT/PLA-ann (annealed) followed by 1.5GNP/4.5CNT/PLA-ann, demonstrated the highest temperatures of the melt crystallization (T_c = 117 °C and 112 °C, respectively) compared to the neat PLA (96 °C). This was clearly due to the very good dispersion of the mixed fillers at those ratios in the PLA matrix (as shown in Figure 2a,b), which could produce a much stronger nucleation effect.

Moreover, the "annealed" aged films demonstrated semi-crystalline behavior with crystallinity of 34%–38% compared to the amorphous-like behavior of the non-annealed aged films with crystallinity of 4%–6%. The strong increase of the degree of crystallinity of the aged nanocomposite films by annealing confirmed that such thermal treatment might be used to recover the aged nanocomposite films incorporating GNPs and CNTs, as increased PLA crystallinity usually leads to improved mechanical properties.

3.4. Reprocessing of Aged Nanocomposite Films

If PLA-based nanocomposite materials have to be further reprocessed, e.g., by hot pressing or recycling by extrusion, then, because of the change in crystallinity, a very different material is going

to be processed [4]. In order to control the materials structure, it is important to study the effect of nucleation agents, such as GNPs and CNTs, on the crystallinity of PLA-based nanocomposite films subjected to melt reprocessing.

In our study, the effect of "melt reprocessing" at 200 °C on the crystallinity of the aged PLA-based composite films was simulated by the DSC second heating run (Figure 5a) and subsequent fast cooling (Figure 5b) within the temperature range of 30–200–30 °C with a heating rate of 20 °C/min. Table 1 summarizes the thermal characteristics and the crystallinity of the "melt reprocessed" films calculated by Equation (1) from the second heating run. As seen in Figure 5a and Table 1, the T_g of the "melt reprocessed" aged films was similar to that of the aged films before reprocessing, but the T_m was slightly enhanced. The reprocessed neat PLA (PLA-re) and the monofiller composite films, as well as the bifiller samples of the equal ratio 3GNP/3CNT/PLA-re did not show cold crystallization in the DSC curves on the second run, and the melting enthalpy was very small, e.g., amorphous materials with crystallinity below 1%. In contrast, the bifiller composites, 4.5GNP/1.5CNT/PLA-re and 1.5CNT/4.5GNP/PLA-re, demonstrated weak cold crystallization processes, as well as a melting enthalpy of fusion (ΔH_m) with peak T_m at 150 °C and crystallinity of 2%–3%, probably due to better dispersion of nanofillers.
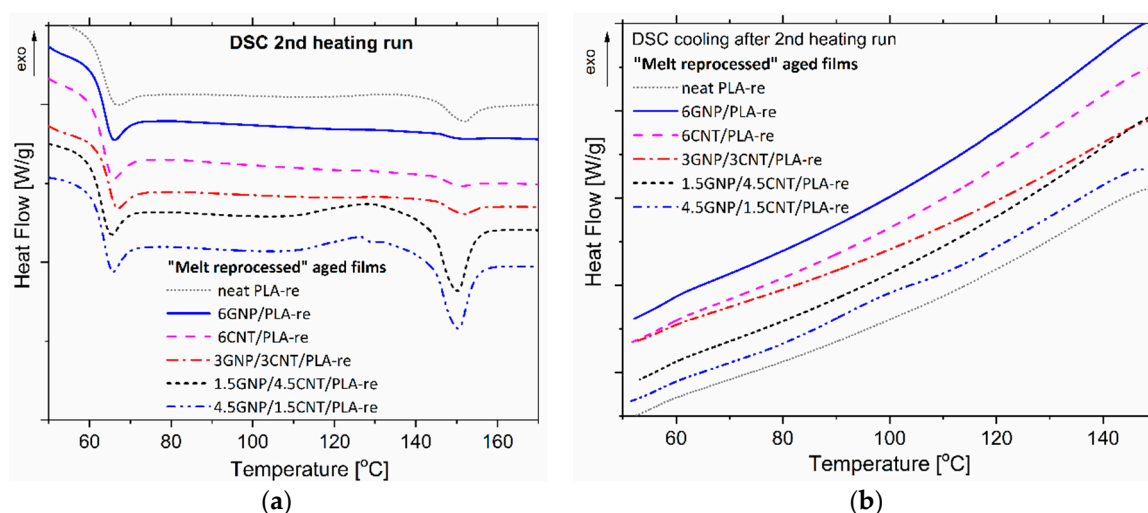

Figure 5. DSC thermograms of "melt reprocessed" aged films and 200 °C: (**a**) DSC second heating run at a rate of 20 °C/min, and (**b**) subsequent fast cooling with a rate of 20 °C/min.

3.5. Thermal Stability and Degradation of Aged Nanocomposite Films

One of the drawbacks of reprocessing PLA-based polymers is the tendency to undergo thermal degradation [9]. In order to minimize the PLA thermal degradation, some authors proposed reinforcement with natural fibers [32]. In our study, we investigated the effects of reinforcement with GNPs, CNTs, and combined fillers on the thermal stability and the degradation of PLA matrix polymer. Thermogravimetric diagrams of weight loss (TG) and their first derivative (DTG) versus temperature are illustrated in Figure 6 for the neat PLA and two example composite films, 1.5GNP/4.5CNT/PLA and 4.5GNP/1.5CNT/PLA, comparing both "aged" and "annealed" samples. The characteristic temperatures, such as the onset of degradation (T_{onset}), the decomposition temperature at 10% weight loss ($T_{10\%}$), and the degradation peak (T_p) for the all studied films are tabulated in Table 2.
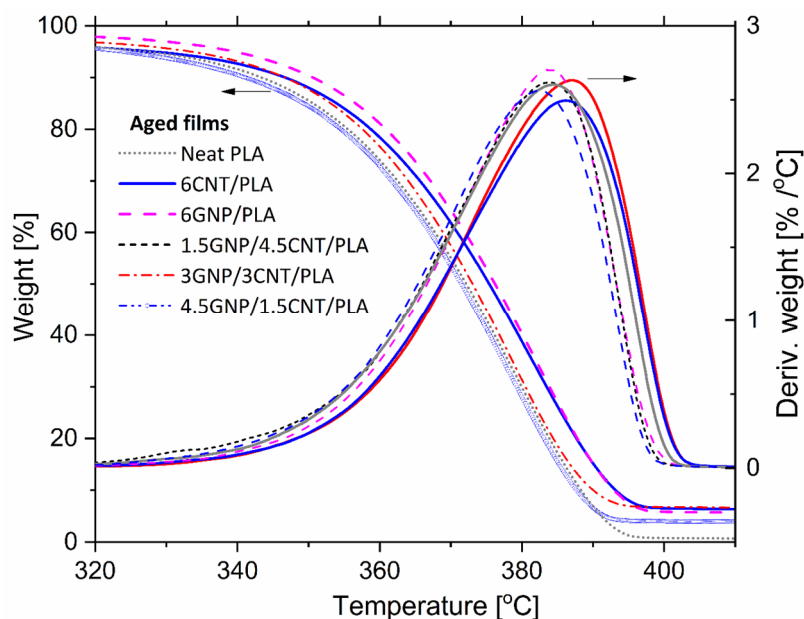
Figure 6. TGA thermograms of weight loss and the derivative versus temperature, comparing the aged bifiller films, 1.5GNP/4.5CNT/PLA and 4.5GNP/1.5CNT/PLA, before and after annealing. Arrows point to the corresponding Y-axis of each set of graphs.

Table 2. Thermal stability (T_{onset}) and degradation peak (T_p) temperatures and mass loss of aged films at 6 wt.% filler. Effect of annealing on thermal characteristics of bifiller composites.

Aged Film after 18 Months Storage	T_{onset} [ºC]	$T_{10\%}$ [ºC]	Peak of Degradation T_p [°C]	Mass Loss at 105 °C [%]	Residue Ash at 500 °C, [%]
Neat PLA	304.5	343.4	378.8	0.23	0.5
6CNT/PLA	308.2	346.7	380.9	0.18	6.0
6GNP/PLA	314.3	350.5	381.9	0.12	5.4
3GNP/3CNT/PLA	313.8	346.5	378.1	0.18	6.3
1.5GNP/4.5CNT/PLA	313.0	344.6	378.0	0.18	5.7
4.5GNP/1.5CNT/PLA	314.4	344.0	378.1	0.15	3.9
1.5GNP/4.5CNT/PLA-ann	310.5	341.3	378.2	0.08	6.3
4.5GNP/1.5CNT/PLA-ann	315.2	340.4	377.0	0.05	3.0

All samples exhibited thermal degradation as a one-stage weight loss within the temperature range of 300–400 °C. The thermograms of the nanocomposites were shifted to higher temperatures compared to those of the neat PLA, which could have been associated with the improved thermal stability by the nanofillers. Particularly, the initial decomposition temperature (T_{onset}) was increased by 4 °C for the composite films with CNTs compared to the neat PLA, while the addition of GNPs shifted up the T_{onset} by about 10 °C. The temperature corresponding to 10% weight loss of nanocomposites was shifted up by 7 °C for the 6GNP/PLA composite compared to the neat PLA (343.4 °C), but the effect of 6CNT/PLA was lower. The results suggested that the addition of GNP nanofiller improved the thermal stability of the nanocomposite films better than CNTs. This could have been associated with the large surface area of graphene nanoplatelets and their high thermal conductivity, which facilitated the heat transfer in the composite and thus reduced the initial degradation. However, the peak of degradation was not affected by the carbon nanofillers at 6 wt.% filler content, thus (T_p) of nanocomposites was similar to that of neat PLA. The effect of annealing on the thermal characteristics of the composite films was insufficient.

The mass loss at 105 °C varied within 0.23% for the neat PLA to 0.12% for the composite films. Annealing reduced the mass loss at 105 °C to 0.05%, probably due to the evaporation of the absorbed moisture in the aged films during long-time thermal annealing (Table 2). The residue ash of the samples

at 500 °C was not equal to the amount of filler that was loaded to the PLA, and this was slightly lower for some samples due to the partial degradation of the filler.

3.6. Nanoindentation Properties of PLA Films after Storage and Thermal Treatment

The nanoindentation analysis was performed in order to study the effect of aging, annealing, and melt reprocessing on nanomechanical characteristics at the three thermal treatment conditions: (i) control aged films; (ii) "annealed" aged film (heated at 80 °C for 4 h); and (iii) "melt reprocessed" aged films (produced by hot pressing at 200 °C). Figure 7 presents the load–depth curves for two example bi-filler aged films, 1.5GNP/4.5CNT/PLA and 4.5GNP/1.5CNT/PLA, as tested before and after annealing and melt reprocessing. The nanoindentation hardness and Young's modulus compared to the respective % crystallinity (from DSC analysis) are reported in Table 3.
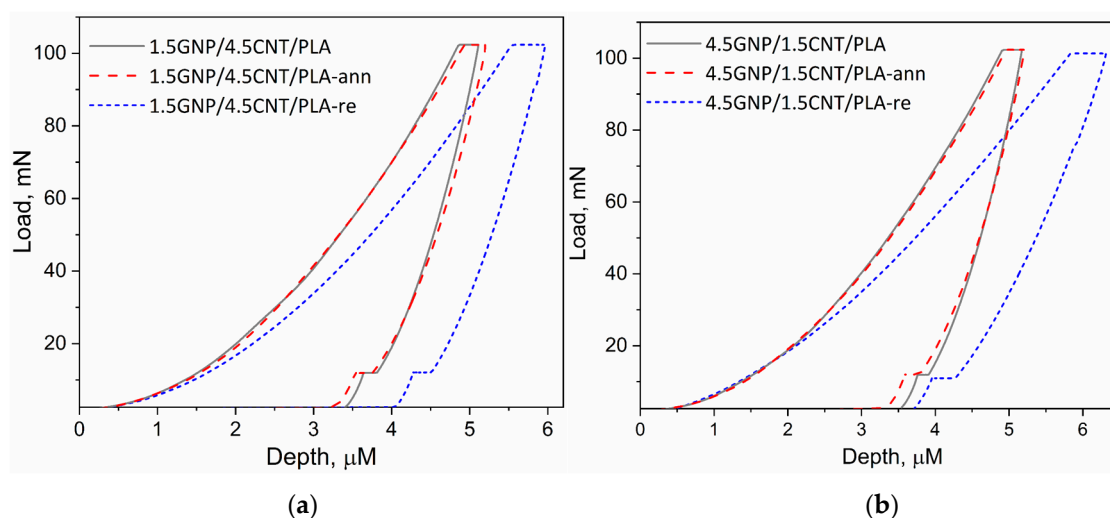

(a)　　　　　　　　　　　　　　　　　　　　　　(b)

Figure 7. Nanoindentation load depth curves of aged bi-filler composite films, 1.5GNP/4.5CNT/PLA (**a**) and 4.5GNP/1.5CNT/PLA (**b**), comparing the control sample, the solid-annealed films (at 80 °C for 4 h), and the melt-reprocessed films (at 200 °C).

Table 3. Nanoindentation hardness and Young's modulus and the crystallinity (χ_{c}.%) of the aged films after 18 months of storage (control) compared to the "annealed" and the "melt-reprocessed" aged films.

Aged Films after 18 Months Storage	Thermal Treatment	Hardness MPa	Young's Modulus, GPa	χ_{c}.%
1.5GNP/4.5CNT/PLA	Control	210 ± 12	3.96 ± 0.15	5.6
1.5GNP/4.5CNT/PLA-ann	Annealed	209 ± 7	3.89 ± 0.07	37.6
1.5GNP/4.5CNT/PLA-re	Melt reprocessed	154 ± 7	3.01 ± 0.32	2.2
4.5GNP/1.5CNT/PLA	Control	211 ± 13	4.13 ± 0.14	5.7
4.5GNP/1.5CNT/PLA-ann	Annealed	209 ± 13	3.82 ± 0.11	33.9
4.5GNP/1.5CNT/PLA-re	Melt reprocessed	150 ± 9	2.08 ± 0.23	3.4

Results showed that the "annealed" aged films had values of hardness and elasticity quite similar to those of the control films before annealing, in spite of the difference in crystallinity, 34%–38% for the "annealed" films and 6% for the control. In contrast, a strong reduction of hardness and Young's modulus appeared for the "melt reprocessed" aged films compared to the control, which could have been associated with their amorphous structure with small crystallinity of 2%–3%, resulting from the melt reprocessing and the subsequent fast cooling. The results showed that, due to the relatively high nanofiller content (6 wt.%), the polymer crystallinity could not be the solitary parameter influencing the surface nanomechanical properties of the composites. The homogeneity of the nanofiller distribution at the surfaces obviously played an important role. Thus, the annealed and the control film produced by

extrusion were expected to have similar homogeneities as the filler at the surfaces. The melt reprocessed films were produced by hot pressing, which may have led to weak separation of polymer and filler phases at the surfaces. This obviously affected the nanoindentation results, which were collected at a low depth of about 3–4 μm.

4. Conclusions

In the proposed work, the PLA based nanocomposite films with 6 wt.% graphene nanoplates, carbon nanotubes, and their mixtures (1.5:4.5, 4.5:1.5 and 3:3 GNP:CNT) were produced by a solution blending technique followed by melt extrusion. The freshly produced films were compared with the aged films after 18 months in storage in a laboratory environment. The effects of annealing (at 80 °C for 4 h) and melt reprocessing (at 200 °C for 15 min) on the crystallinity and the surface mechanical properties were investigated for the studied composite films.

It was found that the crystallinity and the surface mechanical properties depended on the composition and aging, as well as on annealing processes and melt reprocessing.

From the results obtained, the following conclusions can be drawn:

- For the freshly obtained sample, both fillers could act as nucleating agents for PLA crystallization, increasing crystallinity content and preventing the degradation process of the PLA during aging.
- The annealing process of aged films at 80 °C for 4 h followed by slow cooling (as reported) resulted in a strong increase of the degree of crystallinity (34%–38%) compared to the aged films before annealing (3%–6%) and was a procedure that could recover and strongly improve the crystal structure of the aged samples.
- The "melt reprocessing" of aged films at 200 °C followed by fast cooling produced almost fully amorphous films for all samples except the bifiller films, 4.5GNP/1.5CNT/PLA-re and 1.5CNT/4.5GNP/PLA, which showed the presence of very small crystallinity content (2%–3%), probably due to better dispersion of nanofillers.
- The values of the nanoindentation mechanical properties did not depend on the annealing process, whereas they were influenced by melt reprocessing due to the inhomogeneity of the nanofiller at the surfaces produced by hot pressing, with a decrease of the hardness and Young's modulus compared to the control one.

Author Contributions: Conceptualization, R.K.; Data curation, C.S.; Investigation, P.A., T.B. and R.D.M.; Methodology, T.B. and V.A.; Supervision, R.K.; Visualization, R.D.M.; Writing—original draft, R.K.; Writing—review & editing, C.S.

Conflicts of Interest: The authors declare no conflict of interest.

References

1. Ahmed, J.; Zhang, J.X.; Song, Z.; Varshney, S.K. Thermal properties of polylactides. *J. Therm. Anal. Calorim.* **2009**, *95*, 957–964. [CrossRef]
2. Lim, L.-T.; Auras, R.; Rubino, M. Processing technology for poly(lactic acid). *Prog. Polym. Sci.* **2008**, *33*, 820–852. [CrossRef]
3. Pyda, M.; Bopp, R.C.; Wunderlich, B. Heat capacity of poly (lactic acid). *J. Chem. Thermodyn.* **2004**, *36*, 731–742. [CrossRef]
4. Tábi, T.; Sajó, I.E.; Szabó, F.; Luyt, A.S.; Kovács, J.G. Crystalline structure of annealed polylactic acid and its relation to processing. *Express Polym. Lett.* **2010**, *4*, 659–668. [CrossRef]

5. Pan, P.; Zhu, B.; Kai, W.; Dong, T.; Inoue, Y. Polymorphic transition in disordered poly(ʟ-lactide) crystals induced by annealing at elevated temperatures. *Macromolecules* **2008**, *41*, 4296–4304. [CrossRef]

6. Pan, P.; Kai, W.; Zhu, B.; Dong, T.; Inoue, Y. Polymorphous crystallization and multiple melting behavior of poly(ʟ-lactide): Molecular weight dependence. *Macromolecules* **2007**, *40*, 6898–6905. [CrossRef]

7. Martin, O.; Avérous, L. Poly(lactic acid) plasticization and properties of biodegradable multiphase systems. *Polym.* **2001**, *42*, 6209–6219. [CrossRef]

8. Wertz, J.T.; Mauldin, T.C.; Boday, D.J. polylactic acid with improved heat deflection temperatures and self-healing properties for durable goods applications. *ACS Appl. Mater. Interfaces* **2014**, *6*, 18511–18516. [CrossRef] [PubMed]

9. Farah, S.; Anderson, D.G.; Langer, R. Physical and mechanical properties of PLA, and their functions in widespread applications—A comprehensive review. *Adv. Drug Deliv. Rev.* **2016**, *107*, 367–392. [CrossRef]

10. Rasal, R.M.; Hirt, D.E. Toughness decrease of PLA-PHBHHx blend films upon surface-confined photo-polymerization. *J. Biomed. Mater. Res. Part A* **2008**, *88A*, 1079–1086. [CrossRef]

11. Carrasco, F.; Pagès, P.; Gámez-Pérez, J.; Santana, O.O.; Maspoch, M.L. Processing of poly(lactic acid): Characterization of chemical structure, thermal stability and mechanical properties. *Polym. Degrad. Stab.* **2010**, *95*, 116–125. [CrossRef]

12. Du, Y.; Wu, T.; Yan, N.; Kortschot, M.T.; Farnood, R. Fabrication and characterization of fully biodegradable natural fiber—Reinforced poly (lactic acid) composites. *Compos. Part B Eng.* **2014**, *56*, 717–723. [CrossRef]

13. Islam, M.S.; Pickering, K.L.; Foreman, N.J. Influence of accelerated ageing on the physico-mechanical properties of alkali-treated industrial hemp fibre reinforced poly(lactic acid) (PLA) composites. *Polym. Degrad. Stab.* **2010**, *95*, 59–65. [CrossRef]

14. Rasselet, D.; Ruellan, A.; Guinault, A.; Miquelard-Garnier, G.; Sollogoub, C.; Fayolle, B. Oxidative degradation of polylactide (PLA) and its effects on physical and mechanical properties. *Eur. Polym. J.* **2014**, *50*, 109–116. [CrossRef]

15. Liao, R.; Yang, B.; Yu, W.; Zhou, C. Isothermal cold crystallization kinetics of polylactide nucleating agents. *J. Appl. Polym. Sci.* **2007**, *104*, 310–317. [CrossRef]

16. Harris, A.M.; Lee, E.C. Improving mechanical performance of injection molded PLA by controlling crystallinity. *J. Appl. Polym. Sci.* **2008**, *107*, 2246–2255. [CrossRef]

17. Battegazzore, D.; Bocchini, S.; Frache, A. Crystallization kinetics of poly (lactic-acid)-talk composites. *Express Polym. Lett.* **2011**, *5*, 849–858. [CrossRef]

18. Tang, H.; Chen, J.-B.; Wang., J.; Xu, J.-Z.; Hsiao, B.S.; Zhong, G.-J.; Zhong, M. Shear flow and carbon nanotubes synergistically induced nonisothermal crystallization of poly (lactic acid) and its application in injection molding. *Biomacromolecules* **2012**, *13*, 3858–3867. [CrossRef]

19. Xu, Z.; Niu, Y.; Wang, Z.; Li, H.; Yang, L.; Qiu, J.; Wang, H. Enhanced nucleation rate of polylactide in composites assisted by surface acid oxidized carbon nanotubes of different aspect ratios. *ACS Appl. Mater. Interfaces* **2011**, *3*, 3744–3753. [CrossRef]

20. Wu, D.; Cheng, Y.; Feng, S.; Yao, Z.; Zhan, M. Crystallization behavior of polylactide/graphene composites. *Ind. Eng. Chem. Res.* **2013**, *52*, 6731–6739. [CrossRef]

21. Yang, B.; Wang, D.; Chen, F.; Su, L.F.; Miao, J.B.; Chen, P.; Qian, J.S.; Xia, R.; Liu, J.W. Melting and crystallization behaviors of poly(lactic acid) modified with graphene acting as a nucleating agent. *J Macromol. Sci. Part B.* **2019**, *58*, 290–304. [CrossRef]

22. Sodergard, A.; Stolt, M. Properties of lactic acid based polymers and their correlation with composition. *Prog. Polym. Sci.* **2002**, *27*, 1123–1163. [CrossRef]

23. Gao, Y.; Picot, O.T.; Zhang, H.; Bilotti, E.; Peijs, T. Synergistic effects of filler size on thermal annealing-induced percolation in polylactic acid (PLA)/graphite nanoplatelet (GNP) nanocomposites. *Nanocomposites* **2017**, *3*, 67–75. [CrossRef]

24. Botta, L.; Scaffaro, R.; Sutera, F.; Mistretta, M.C. Reprocessing of PLA/Graphene Nanoplatelets Nanocomposites. *Polymers* **2018**, *10*, 18. [CrossRef] [PubMed]

25. Tsuji, H.; Ikada, Y. Properties and morphologies of poly(ʟ-lactide): I. Annealing condition effects on properties and morphologies of poly (Llactide). *Polymer* **1995**, *36*, 2709–2716. [CrossRef]

26. Perez-Fonseca, A.A.; Robledo-Ortíz, J.R.; González-Núñez, R.; Rodrigue, D. Effect of thermal annealing on the mechanical and thermal properties of polylactic acid–cellulosic fiber biocomposites. *J Appl Polym Sci.* **2016**, *133*, 43750. [CrossRef]

27. Ivanov, E.; Kotsilkova, R.; Xia, H.; Chen, Y.; Donato, R.K.; Donato, K.; Godoy, A.P.; Di Maio, R.; Silvestre, C.; Cimmino, S.; et al. PLA/graphene/MWCNT composites with improved electrical and thermal properties suitable for FDM 3D printing applications. *Appl. Sci.* **2019**, *9*, 1209. [CrossRef]

28. Batakliev, T.; Petrova-Doycheva, I.; Angelov, V.; Georgiev, V.; Ivanov, E.; Kotsilkova, R.; Casa, M.; Cirillo, C.; Adami, R.; Sarno, M.; et al. Effects of graphene nanoplatelets and multiwall carbon nanotubes on the structure and mechanical properties of poly (lactic acid) composites: A comparative study. *Appl. Sci.* **2019**, *9*, 469. [CrossRef]

29. Oliver, W.C.; Pharr, G.M. Measurement of hardness and elastic modulus by instrumented indentation: Advances in understanding and refinements to methodology. *J. Mater. Res.* **2004**, *19*, 3–20. [CrossRef]

30. Cimmino, S.; Karasz, F.E.; Macknight, W.J. Miscibility and phase behavior in atactic polystyrene and poly(o-chlorostyrene-co-p-chlorostyrene) blends: Effect of polystyrene molecular weight and copolymer composition. *J Polym Sci. Part B.* **1992**, *30*, 49–59. [CrossRef]

31. Struik, L.C.E. Physical Aging in Amorphous Polymers and Other Materials. Ph.D. Thesis, TU Delft, Delft, The Netherlands, November 1977.

32. Fan, Y.; Nishida, H.; Shirai, Y.; Tokiwa, Y.; Endo, T. Thermal degradation behavior of poly(lactic acid) stereocomplex. *Polym. Degrad. Stab.* **2004**, *86*, 197–208. [CrossRef]